The significance of stromal collagen organization in cancer tissue: an in depth discussion of literature

Zunder, S.M.; Gelderblom, H.; Tollenaar, R.A.; Mesker, W.E.

Critical Reviews in Oncology / Hematology 151 (2020) 102907

Contents lists available at ScienceDirect

Critical Reviews in Oncology / Hematology

journal homepage: www.elsevier.com/locate/critrevonc

Review

The significance of stromal collagen organization in cancer tissue: An in-depth discussion of literature

Stéphanie M. Zunder[a,b], Hans Gelderblom[b], Rob A. Tollenaar[a], Wilma E. Mesker[a,*]

[a] Department of Surgery, Leiden University Medical Centre, Albinusdreef 2, 2300 RC, Leiden, The Netherlands
[b] Department of Medical Oncology, Leiden University Medical Centre, Albinusdreef 2, 2300 RC, Leiden, The Netherlands

ARTICLE INFO

Keywords:
Cancer
Tumor stroma
Collagen
Organization
Review

ABSTRACT

It has become clear that carcinogenesis goes beyond tumor cell biology. Cancer research has acknowledged the importance of biological functions of the tumor-microenvironment, wherein not only cellular components seem to hold valuable information but also structural components like collagen fibers. Several studies have focused on the significance of stromal collagen fiber organization and reported on its role in cancer progression, invasiveness and treatment response. In this review, we discuss the different imaging methods for stromal collagen organization, followed by an in-depth discussion of current literature on in-vitro and animal experiments and human studies, highlighting its importance with respect to cancer progression, prognosis and prediction. We can conclude that collagen organization contains valuable information with regard to metastatic potential and clinical outcomes in cancer. However, the significance of an aligned versus disorganized collagen morphology differs between cancer types, implying more research is necessary before steps towards clinical implementation can be made.

1. Introduction

Cancer remains a worldwide health burden and leading cause of death, with an estimated 18.1 million new cases and 9.6 million deaths in 2018 (Bray et al., 2018). Despite the frequent occurrence, the biology of this disease is far from being completely unraveled. Initially cancer research focused on tumor cell biology, wherein the so-called hallmarks of cancer emphasized cancer cell associated biological aspects (i.e. sustained proliferative signaling, insensitivity to growth suppressors, cell death resistance, limitless replicative potential, sustained angiogenesis and tissue activation, invasion and metastasis) (Hanahan and Weinberg, 2000). However, this concept was revised almost a decade later (Hanahan and Weinberg, 2011), as the complexity of tumorigenesis had been recognized as a bidirectional communication between cancer cells and certain cell types within the tumor microenvironment. This process shares many similarities with wound healing, wherein the presence of dense collagenous stroma (i.e. desmoplastic response) around the tumor cells is the result of a complex interaction between the hosts 'stromal cell response against invading cancer cells, by activation of various inflammatory cells and growth factors such as vascular endothelial growth factor (Dvorak, 2015; Ribatti and Tamma, 2018). Extensive research is ongoing in this field, in order to gain more understanding in the biological functions of the tumor microenvironment. In the past years, numerous studies have been published focusing on the significance of stromal architecture and collagen organization with regard to cancer progression, invasiveness and treatment response. Here, we give an overview of literature investigating this stromal organization, highlighting its significance within cancer progression,

Abbreviations: 3D, three-dimensional; A:I, ratio anisotropic to isotropic ratio; ANN, artificial neural network; BIF, basic image features; CAFs, cancer associated fibroblasts; CRC, colorectal cancer; CRPC, castration-resistant prostate cancer; DCIS, ductal carcinomas in situ; DFS, disease-free survival; DSS, disease-specific survival; EAC, esophageal adenocarcinoma; ECM, extracellular matrix; EMT, epithelial–mesenchymal transition; ER, estrogen receptor; F/B, ratio forward to backward signal ratio; GLCM, gray-level co-occurrence matrix texture analysis; GLEM, gray level entropy matrix texture analysis; H&E, hematoxylin and eosin; HGS, high-grade serous; HNSCC, head & neck squamous cell carcinoma; IBC, invasive breast cancer; IDC, invasive ductal breast carcinoma; IHC, immunohistochemical staining; LBP, local binary patterns; MP-FRAP, multiphoton fluorescence recovery after photobleaching; MPLSM, multiphoton laser scanning microscopy; MPM, multiphoton microscopy; NSCLC, non-small cell lung cancer; OCT, optical coherence elastography/tomography; OS, overall survival; OSF, oral submucous fibrosis; PDAC, pancreatic ductal adenocarcinoma; PLOD2, lysyl hydroxylase 2; PR, progesterone receptor; PSC, pancreatic stellate cells; PSR-POL, picrosirius red-polarization; SCC, squamous cell cancer; SHG, second harmonic generation; TACS, tumor-associated collagen signature; TEM, Transmission Electron Microscope; TMA, tissue microarray; TPEF, two-photon fluorescence; TTD, total traveled distance; WT, wildtype

* Corresponding author at: Department of Surgery, Leiden University Medical Centre, Albinusdreef 2, 2300 RC Leiden, The Netherlands.
E-mail address: W.E.Mesker@lumc.nl (W.E. Mesker).

https://doi.org/10.1016/j.critrevonc.2020.102907
Received 19 December 2019; Received in revised form 9 February 2020; Accepted 10 February 2020

Table 1
Basic principles of visualization methods for stromal collagen organization.

Method	Basic principle	Required tissue staining	Microscopy	Advantage	Disadvantage
Semi-visual microscopy	- Manual drawing of lines alongside the stromal fiber orientation on digitalized tissue slide. - Vector orientation and SD are used for calculation of stromal organization score.	H&E AZAN trichrome	Conventional light Image J (open-source software tools for collagen organization)	- Inexpensive - Easily integrated in routine practice	- Observer dependent method - Labor intensive
Masson's trichrome	- Masson's staining allows better discrimination between collagen and connective tissue components.	Masson's trichrome	Conventional light Laser scanning	- Inexpensive - Application with different visualization techniques	- Additional staining
Picrosirius red staining	- Picrosirius binds to collagen and enhances natural birefringent properties of collagen molecules for better microscopic visualization.	Picrosirius red	Polarized light	- Inexpensive - Enhances visualization of collagen fiber orientation	- Additional staining - Only specific for collagen when combined with polarized light
Second harmonic generation imaging	- Laser pulse passes through non-centrosymmetric material resulting in non-linear, second-order polarization. - Polarization anisotropy is used for structural analysis of collagen organization.	Not required, but optional	Laser scanning Combined with open-source software tools for collagen organization (i.e. CurveAlign, CT-FIRE)	- No additional staining required - Direct visualization of individual fibrillar collagen fibers	- Expensive - Elaborate equipment
Two-photon microscopy and fluorescence	- High flux excitation photons are produced by a laser. - Two low-energy photons are simultaneously absorbed by a fluorophore, which causes a higher-energy excitation and consequent fluorescent emission.	Fluorophore	Laser scanning	- Easily available in routine image analysis packages	- Additional staining - Less sensitive to small differences within tissue
Wavelet artificial neural network based analysis	- Computational method performs multifactorial analyses based on layers of computing nodes that operate as a non-linear summing device, to perform correct data classification / prediction.	NA	Wavelet transformation analysis which can be applied on various types of (microscopical) images	- No additional staining required	- Dependent on clear tumor-cell boundary to generate correct vector
Gray level entropy matrix texture analysis	- Second-order texture features are computed from statistical distributions of observed intensity combinations at specified positions relative to each other in an image.	NA	Statistical texture analysis which can be applied on various types of (microscopical) images	- No additional staining required - Semiautomated and quantitative analyses - Easy to implement	- Dependent on visual separability of textures - Sensitive to - sample size
Optical coherence elastography/ tomography	- Low coherence light captures resolution and 2D / 3D images derived from optical scattering materials.	Not required, but optional	NA	- No additional staining required - Realtime imaging - Integration in scopes / handheld scanners	- Sensitive to motion artifacts - Lengthy computational processing

Abbreviations: SD standard deviation, H&E hematoxylin and eosin, NA not applicable, 2D two-dimensional, 3D three-dimensional.

prognosis and prediction. We will first describe the different techniques used to visualize the stromal collagen organization, followed by an in-depth discussion of current in vitro and animal experiments, and realization of proof of principle in human studies.

1.1. Visualization methods

Numerous visualization methods are available for quantification and characterization of stromal collagen organization within cancer tissue, ranging from conventional to highly sophisticated microscopy techniques. In the next section we will elaborate on the methodology of these techniques. For a summary and illustration of frequently used histological staining's and microscopic visualization methods, see Table 1 and Figure S1.

1.1.1. Semi-visual microscopy

Conventional microscopy could be considered the easiest applicable and most cost-effective method for determination of collagen organization, since it can be easily incorporated in routine diagnostic workflows. To capture the collagen organization using this method, intratumoral regions (surrounded by neoplastic cells at all corners) are selected in three individual hematoxylin and eosin (H&E)-stained tumor tissue slides. Using ImageJ (Image Processing and Analysis in Java), approximately 10–15 straight lines are drawn onto the image, alongside the stromal fiber orientation. Subsequently, the mean orientation of these vectors and the standard deviation of the orientation are determined as measure for stromal fiber network organization of the tumor. Wherein a high standard deviation indicates broad distribution, hence disorganized stroma and a low value indicates radially organized stroma (Fig. 1, Figure S1A, Figure S2). Adding AZAN trichrome staining, which highlights the collagen component of tissue, did not improve this method. Comparison of stromal organization scores for both methods ($n = 51$) revealed a good correlation ($r = 0.806$), indicating that H&E-stained slides are sufficient and adequate for the stromal organization scoring using this method (Dekker et al., 2015).

1.1.2. Masson's trichrome

Another staining method, applied for connective tissue visualization is the Masson's trichrome stain. This three color staining protocol is based on a purple (hematoxylin) nuclear stain, a red (mix of xylidin ponceau and acid fuchsin) cytoplasmic stain and a light green or aniline blue collagen fiber stain, wherein the discrimination between collagen and other connective tissue components is linked to a difference in permeability (Figure S1E) (https://www.histalim.com/home/activities/our-services/histology/masson-trichrome/https://www.histalim.com/home/activities/our-services/histology/masson-trichrome/). A study assessing the agreement and reliability of collagen bundle orientation measurements between different staining and microscopic techniques, revealed Masson's trichome staining with light microscopy was equivalent to picrosirius red staining with polarized microscopy and H&E-confocal with microscopy (Marcos-Garces et al., 2017).

1.1.3. Picrosirius red staining with polarized light microscopy

The picrosirius red stain (also known as "Sirius red" stain) is a more widely applied histochemical technique for selectively highlighting and visualizing collagen networks. This inexpensive method relies on the birefringent properties of collagen molecules. Otherwise explained, when collagen fibers are hit by light, this is refracted into two rays which travel at a different speed and vibration direction oriented at 90° to each other. When picrosirius red (an elongated birefringent molecule) is bound to collagen it positioned parallel to the collagen, thereby increasing the natural birefringence. These complexes of picrosirius red-bound fibrillar collagens can be detected under polarized light, wherein they have a bright appearance which set them apart from the other tissue which remain dark or black (Figure S1B - C) (Rittie, 2017). This picrosirius red-polarization (PSR-POL) method has a good correlation with another collagen-imaging method, namely second harmonic generation (SHG) imaging. However, benefits of PSR-POL over SHG are its ability of higher detection of fiber counts, length, alignment, straightness and width (Drifka et al., 2016a). See Table 1 for a detailed overview of the individual advantages and disadvantages of the individual visualization methods.

1.1.4. Second harmonic generation imaging

SHG imaging is a high-resolution laser scanning microscopy technique, which produces quantifiable images of collagen fiber networks in stained and unstained tissue slides. In 1961, the concept of the second harmonic of the original light was first demonstrated by Franken et al, as they observed that pulses of deep red ruby laser light through a quartz crystal produce ultraviolet light (Franken, 1961). Hereafter, others followed to formulate basic principles of this SHG and other nonlinear optics (Bloembergen, 1965), which eventually lead to the concept of implementation of SHG in scanning microscopes and the first biological SHG imaging experiments in 1986 (Dolino, 1973; Gannaway and Sheppard, 1978; Freund et al., 1986). In short, SHG imaging relies on an intense laser pulse passing through materials with a non-centrosymmetric environment. Upon this, the laser field undergoes a nonlinear, second-order polarization, resulting in a signal at half the wavelength (at doubled frequency) of the original light entering the material. SHG is a coherent process, wherein signals are mainly collected in a forward direction. The forward to backward signal ratio (F/B ratio) is herein dependent on the sample traits. For instance, increased turbidity leads to more backward scatter. The polarization anisotropy that is produced by SHG, can be used to determine the degree of protein organization within tissue, as well as axial and radial symmetries and absolute orientation (Figure S1D) (Mohler et al., 2003). Most SHG imaging setups will use a laser scanning microscope with a titanium sapphire mode-locked laser to serve as an excitation source. Despite of the promising results in tissue and collagen network characterization (detailed study results in section in vivo studies -humans) (Conklin

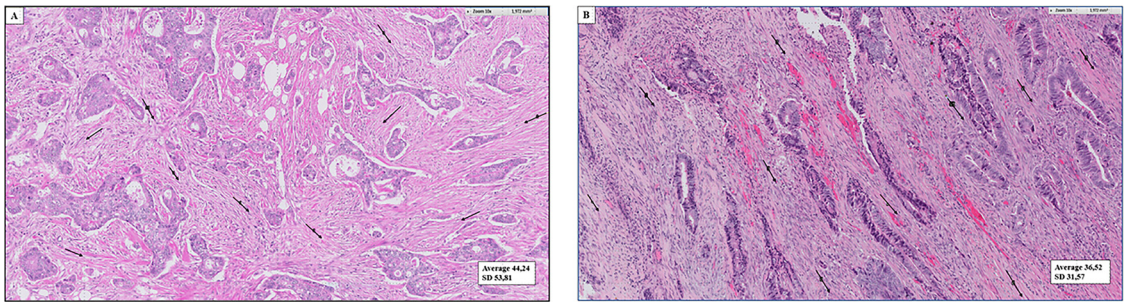

Fig. 1. Hematoxylin and Eosin colon cancer tissue slides.
(A) Example of colon cancer tissue with disorganized stroma.
(B) Example of colon cancer tissue with aligned stroma.

et al., 2011; Hanley et al., 2016; Drifka et al., 2015; Provenzano et al., 2006; Zhou et al., 2017), SHG imaging is currently not implemented in routine tissue diagnostics due to the complexity of this sophisticated system as well as the technical demands and expenses.

1.1.5. Two-photon microscopy and fluorescence

Another non-linear microscopy method is two-photon fluorescence (TPEF), also referred to as two-photon laser scanning microscopy, multiphoton microscopy (MPM) or multiphoton laser scanning microscopy (MPLSM). A technique which offers increased image depth analysis by using infrared light which minimizes scattering in the tissue and suppression of background signals due to the multiphoton absorption. This offers superior imaging compared to confocal microscopy, but at limited phototoxicity. In stroma, the TPEF signals mainly arise from the elastin within the stroma. The principle of this method was first described by Maria Göppert-Mayer in 1931 (Goeppert-Mayer, 1931). In TPEF, a laser is focused, causing photons to become more crowded and enhancing the probability of simultaneous absorption of two photons by a fluorophore. As this simultaneous absorption occurs, it leads to emission of one photon to a higher energy state causing selective excitation of fluorophores in a sample (Figure S1F). To achieve a significant number of two-photon absorption events, the density of photons must be around one million times higher than is required to generate the equivalent number of one-photon absorptions. This power can only be achieved by using focusing mode-locked (pulsed) lasers (Denk et al., 1990; Denk and Svoboda, 1997).

1.1.6. Other methods

Other more sparsely applied methods in collagen network visualization are; wavelet artificial neural network (ANN) based analysis (Mukherjee et al., 2006; Paul et al., 2005), gray level entropy matrix (GLEM) texture analysis, multi-scale basic image features (BIF) and local binary patterns (LBP) (Jia et al., 2014; Kirkpatrick et al., 2007; Reis et al., 2017), and optical coherence elastography/tomography (OCT) (Watson et al., 2014; Yuting et al., 2018). In summarization, artificial neural network analysis is a computational methodology which performs multifactorial analyses, wherein a ANN model contains layers of interconnected computation nodes that operate as a non-linear summing device. The network can subsequently be trained to predict, classify or recognize data features, like for instance collagen organization on Transmission Electron Microscope (TEM) images (Mukherjee et al., 2006; Paul et al., 2005; Dayhoff and DeLeo, 2001). In GLEM texture analysis, the number of gray levels within a digitalized microscopy image is reduced by requantization, whereafter the local entropy within the window is computed and centered around a pixel with a certain gray-level value, which is based on the gray-level distribution within that specific window. The GLEM which is computed from the complete image, is visualized as surface plots and gray-scale. The local entropy values are based on estimated gray-level distributions, consequently homogenous structures will have low entropy levels, whereas inhomogeneous structures will have high levels (Jia et al., 2014; Nielssen et al., 2008). OCT is a method which application is under great development with respect to cancer imaging. This technique is based on coherent light to capture resolution, 2D and 3D images from within optical scattering media, like tissue (Wang and Larin, 2015). BIF and LBP are alternative statistical texture analyses methods, since these are not widely applied, it goes beyond the scope of this paper to provide a detailed description. Therefore we would refer to literature for more details (Reis et al., 2017).

2. Discussion of literature

2.1. Stromal collagen organization

As previously referred to, tumorigenesis is currently considered as an interplay between tumor cells and the surrounding stroma with its stromal host cells (Hanahan and Weinberg, 2011; Liotta and Kohn, 2001; Hanahan and Coussens, 2012). In order to recognize the pathophysiology and implications of collagen organization alterations in carcinogenesis, fundamental research models are necessary. Only hereafter, it is possible to validate and translate these findings to human studies and recognize which factors have clinical implications in cancer treatment. See Table S1 for a summarized overview of the subsequently described studies.

2.1.1. In vitro studies

In order to understand the mechanisms involved in stromal organization in relation to tumor invasion and progression, research in controlled environments offers great opportunities to study cell motility and subsequent effects on collagen fibers without interference of uncontrolled extrinsic signals. The first study reporting on extracellular matrix (ECM) reorganization comes from Friedl et al. In this study, cell-to-matrix interactions of migrating MV3 melanoma cells were evaluated in three-dimensional (3D) collagen lattices. The authors demonstrated that increased collagen concentrations influenced collagen fibers, leading to increased fiber density as well as decreasing of the mean distance between collagen fibers. More interestingly, they also observed progressive matrix reorganization after 24 h incubation, whereby the original pattern of matrix texture and pores between fibers was practically completely replaced by an irregular distribution pattern of random and aligned fibers in close proximity with the interacting MV3 cells. According to the authors, this could contribute to tumor cell progression by the observation that following collagen fiber attachment and cell polarization, cell migration paths followed the presence of stretched fiber strands or preexisting tube-like paths of least resistance in the fiber network. This implicated that contact–stimulated migration is involved (Friedl et al., 1997). This concept, referred to as lamellipodia, was also evaluated by Lepzelter et al using 3D extracellular matrix models, wherein was observed that a substantial part of persistence was directly dependent on the physical environment (i.e. available moving directions and steric hindrance), rather than indirectly dependent on the environment through the biochemical feedback that occurs in cell motility. Moreover, the models revealed that highly aligned matrix should produce smaller cell displacement speed, due to the fact that lamellipodia takes longer to search an empty area ahead of the cell, which is subsequently offset by increased persistence (Lepzelter and Zaman, 2014). Contrary to these discoveries, the 3D invasive ductal breast carcinoma (IDC) cell migration models of Riching et al did not observe effects on migration speed of cancer cells models with altered alignment or collagen concentrations. However, in accordance to Lepzelter et al, they did observe enhanced directional migration persistence within aligned matrices, which was unrelated to increased matrix stiffness. This alignment was alternatively referred to as a tumor-associated collagen signature (TACS) (Riching et al., 2014). Previous reports demonstrated that, in particular, the deposition of aligned collagen with a perpendicular orientation to the tumor boundary (TACS-3) has proven to create migrational highways for tumor cells in vivo (Provenzano et al., 2006), along with correlation to increased invasion and metastasis in animal models (Provenzano et al., 2008). Additionally, Riching et al reported limited protrusions and longer cells within aligned collagen, suggesting that this is a mechanism by which alignment serves to increase persistence and facilitates greater travel distances. Unlike the former collagen gel-based techniques, Burke and colleagues emphasized their research on exploring the relation of fiber microstructure (indicated by F/B ratio) to tumor cell motility. Based on an in vivo model, 4T1 murine mammary adenocarcinoma cells were chosen as cell line for further in vitro analysis (Burke et al., 2013). In order to study cell motility responses to differences in microstructures, fibrillogenesis of the collagen gels was altered using different methods. The models demonstrated, when large amounts of cells (3×10^5 cells/mL of media) were added (after 3 days), significant increases in F/B ratio were induced on fibers in near proximity of tumor cell clusters,

causing them to become more straightened and perpendicularly protruding. To insure true cell motility analysis, further experiments were performed by adding lower cell concentrations and earlier imaging (3 h vs. 3d). Analysis showed an overall significant effect of F/B category on total traveled distance (TTD) of cells ($p < 0.05$), whereby post-hoc analysis demonstrated that TTD on the two highest F/B category gels (F/B = 8.13 ± 0.16; F/B = 10.60 ± 1.08) was significantly greater than on the two lowest F/B categories (F/B = 2.81 ± 0.29; F/B = 6.20 ± 0.14; $p < 0.05$), which could be related to the efficiency of cells to pull themselves along fibers. Cell velocity analysis confirmed this hypothesis, revealing significantly higher cell velocity in the highest F/B category gels compared to the lowest F/B categories. Additional correlation analysis demonstrated significant positive relationships between F/B ratio and two out of three motility parameters; average cell velocity ($p < 0.05$), maximum cell velocity ($p < 0.05$) and TTD ($p = 0.06$) (Burke et al., 2015a). Since the observations in this study match previous results, wherein humane IDC tumors with higher F/B ratios produced more lymph node metastases compared to tumors with lower F/B ratios,(Burke et al., 2013) these gel experiments suggest that the in vitro microstructure (i.e. F/B ratio) does influence tumor cell motility and metastatic potential. Exploring how modulation of substrate stiffness influences fiber alignment by cancer-associated fibroblasts (CAFs), Malik et al cultured humane cancer-associated fibroblasts at high density on collagen-I polyacrylamide gels allowing them to produce cell-derived ECM. They demonstrated a biphasic fiber alignment with more than 60% fiber alignment on gels with a pathological stiffness (~7 kPa) compared to 30% on physiologically stiff gels (~1.5 kPa) (Malik et al., 2018).

Based on the aforementioned in vitro studies, we are provided with great insights in mechanisms involved in cancer cell motility and its effects in relation to collagen architecture and organization. However, due to the controlled nature of these models, the concepts are not readily translatable to in vivo models.

2.1.2. *In vivo studies — animals*

With the transition from in vitro to experimental animal models we are one step further to clinical translation and application of stromal reorganization in practice. In the publication of Riching, reference is made to alignment by means of tumor-associated collagen signatures. Provenzano et al first revealed these signatures in a study evaluating epithelial and tumor-stromal interactions in a breast cancer mice model, to get insights in local cell invasion mechanisms during carcinogenesis. Herein, multiphoton excitation-SHG imaging revealed three distinct TACS to characterize tumors, namely; TACS-1, the presence of dense collagen fibers indicated by an increased signal intensity in the region surrounding the tumor; TACS-2, characterized by the presence of straightened ("taut") collagen fibers stretched around the tumor, indicating growth leading to increased tumor volume; and lastly TACS-3, the presence of radially aligned collagen fibers which facilitate invasion and may be indicative of invasive and metastatic tumor growth potential Provenzano et al. (2006). By using picrosirius red staining combined with high magnification scanning electron microscopy, they demonstrated within normal mammary gland models, that collagen fibers are wrapped around the ductal structures in an organized manner surrounding epithelial cells and are additionally able to wrap individual cells in multiple directions, which could suggest a role as an anchoring and restraining structure. Further investigation into TACS-3 demonstrated that in tumor regions undergoing growth and invasion, collagen fibers aligned perpendicular to the tumor. The authors hypothesize that this realignment emerges through contractile and morphogenic events from the cells at the tumor boundaries, in order to organize the ECM and prepare for local invasion. This was supported by several additional analyses of collagen structures within regions of invading cells, whereby all models revealed that local tumor invasion occurred solely where collagen fibers were radially aligned from the tumor in direction of tumor cell invasion. A type-I collagen model demonstrated direct contact between radially reorganized collagen fibers and invading cells, suggesting that tumor cells are able to reorganize collagen matrices de novo, in order to facilitate invasion (Provenzano et al., 2006). As it has been demonstrated that desmoplasia, a feature often seen in more aggressive tumors, consists of increased deposition of fibrillar collagens like collagen-I, which by itself leads to stiffening of the ECM, as well as by alignment (Riching et al., 2014; Butcher et al., 2009; Keely, 2011), Barcus et al emphasized on the significance of ECM stiffness in breast cancer progression. By orthotopically transplanting clonal green fluorescent protein (GFP)-labelled prolactin-induced ERα+ mammary tumor cell lines into syngeneic wildtype (WT ($n = 14$)) or heterozygous mutant collagen-I female mice (*Col1a1*$^{tmJae/+}$, mCol1a1 ($n = 14$)), a model with increased collagen-I was constructed (Barcus et al., 2017). In correspondence with the models from Provenzano, PSR-POL microscopy revealed that in mCol1a1 mice, dense collagen fibers were aligned with tumor projections whereas in WT mice the fibers were wrapped around the tumor edges, similar to collagen fibers in non-aggressive tumors (Conklin et al., 2011; Provenzano et al., 2006). SHG imaging combined with alignment analysis demonstrated a significant difference in alignment between tumors of WT recipients, wherein collagen fibers were aligned to each other and parallel to the tumor edge, whereas in tumors of mCol1a1 recipients, the fibers were less orientated ($p < 0.0001$) with many perpendicular to the tumor bulk or aligned with protrusions into the fat pad. This indicates the ECM can interact with hormonal signals in order to induce metastatic potential in ERα+ breast cancers (Barcus et al., 2017). Evaluating microscopic changes associated with disease development in ovarian cancer, Watson et al were able to demonstrate alterations in the ovarian microstructure, even before macroscopic changes were visible. SHG imaging ($n = 44$) revealed that with progression from normal ovaries to other phenotypes, the collagen microstructures altered from thin, linear and tightly net-like packed fibers in normal ovarian tissue and cystic tumors, however in the latter with more abundant than normal appearance of collagen, to fewer collagen with fibers that appeared tangled and spread-out in tubular hyperplasia and fibrosarcoma tumors (Watson et al., 2014). Although these results are promising and suggest a combination of optical coherence tomography-MPM systems could be useful in early detection of ovarian cancer, a limitation is the absence of adenocarcinomas in this study, causing it to not fully represent the clinical situation. Aforementioned studies have demonstrated within different tumors types, carcinogenesis is associated with alterations in collagen organization, with respect to disease progression and invasion. Where these studies mainly focus on the overall effects on the ECM, other studies highlight the purpose of specific receptors and/or proteins within ECM remodeling. For instance, Navab et al studied the role of integrins in non-small cell lung cancer (NSCLC), since these have been indicated as factors in tumor proliferation, migration, invasion and act as multifunctional receptors in tumor stroma (Barczyk et al., 2010; Desgrosellier and Cheresh, 2010). Specifically looking into α11β1 expression (i.e. stromal cell-specific receptor for fibrillar collagens), SHG imaging of tumor xenografts in a knockout mice model revealed that loss of α11 expression was significantly correlated with decreased ECM stiffness and collagen organization and consequently with less tumorigenicity (Navab et al., 2016). Du et al also evaluated a specific marker within NSCLC, namely lysyl hydroxylase 2 (PLOD2). An enzyme which is an important collagen synthetase that is able to induce collagen reorganization and has proven to be prognostic in several cancers (Chen et al., 2015; Gilkes et al., 2013). In their study, the effects of PLOD2 on ECM and tumorigenesis were further explored using a knock-out metastasis model. The authors confirmed that the metastatic potential decreased with silencing of PLOD2, along with the observation of reorganization of collagen. Namely, within PLOD2 knock-out tumors, picrosirius red and Masson's trichrome staining revealed less alignment of collagen fibers compared to the control group, hereby hindering the formation of an aligned "pathway" for cancer cell migration. Thus suggesting that PLOD2 induces collagen reorganization in NSCLC in

order to promote metastasis.

Abovementioned studies prove that microscopic examination of tumor collagen organization may provide a credible prognostic signature relevant for clinical evaluation, but also suggest a potential for development of therapeutic strategies, specifically targeting the tumor microenvironment. Stylanianopoulos et al explored this issue, by developing a mathematical approach for calculation of diffusion coefficients of nanoparticles and macromolecules in collagenous tissues, in order to study the effect of collagen fiber organization on diffusion anisotropy. They applied a network generation algorithm, wherein diffusing particles are randomly distributed in a 3D fiber network and moved stepwise inside the fiber medium, subsequently calculating a diffusion coefficient based on Stokesian dynamics (Phillips, 1989). Analyses on four network structures ranging from nearly isotropic to aligned, demonstrated that particles diffusion speed significantly increased with alignment of fiber networks. However, the overall diffusion coefficient was independent of pore size distribution and network orientation. To support the mathematical predictions, SHG imaging and single point multiphoton fluorescence recovery after photobleaching (MP-FRAP) measurements were performed in collagen gel and tumor tissue models. In accordance with the mathematical predictions, the aforementioned measurements on gel models, ruled out a correlation between hindered diffusivity and fiber alignment. Line-FRAP measurements were used to investigate the effect of fiber alignment on diffusion anisotropy in a soft tissue sarcoma xenograft model. The results showed that the diffusion coefficient was 1.5 times higher in highly aligned collagen fibers parallel to the fiber direction compared to perpendicular arranged fibers (Stylianopoulos et al., 2010). This illustrates a promising aspect of stroma alignment within optimizing drug delivery strategies in cancer treatment.

2.1.3. In vivo studies – humans

Here, we reach the phase of translational research wherein the theories and results from in vitro and animal experiments are put to test in human models.

Ovarian cancer. Several studies have been performed in ovarian cancer, evaluating the changes in collagen organization with respect to tumor development and progression. Zhu et al investigated the distribution of type III collagen at the epithelial-stroma junction, in different ovarian cancers ($n=77$). Second to collagen-I, collagen-III is also a precursor of the most abundant collagens deposited in soft tissues (Prockop et al., 1979). Using an immunohistochemical staining (IHC) against the PIIINP-domain of type III collagen, the authors found that within malignant tumors the staining intensity of PIIINP was significantly less striking ($p < 0.001$) compared to benign tumors. More interestingly, they observed an irregular organization of collagen fibers at the epithelial-stromal junction in malignant neoplasms, whereas in benign neoplasms the distribution was regular with fine fibers in close proximity, tightly arranged in a fibrillar pattern ($p < 0.001$). The authors suggest that this disintegration could be due to proteolytic enzymes activity during tumorigenesis, although reorganization was also observed in stromal regions distant from malignant cells (Zhu et al., 1993). Using more sophisticated imaging techniques, Kirkpatrick et al, also demonstrated architectural differences between benign, high-risk and malignant ovarian biopsies. By assessing the epithelial surface and underlying stroma with TPEF and SHG, they found that in normal ovarian tissue, collagen fibrils alter with age. Having a linear, long and straight arrangement in young patients, to a more curved and diffuse one in older women. These qualitative appearances were confirmed by gray-level co-occurrence matrix (GLCM) texture analysis in a small cohort ($n_{30\text{-}49}=7$; $n_{50\text{-}60}=4$; $n_{>60}=10$; $p=0.02$). Regarding collagen alterations in malignant tissue, the authors compared biopsies from a group of postmenopausal women ($n=4$ normal; $n=5$ cancer), wherein the cancer tissue displayed loss of well-defined fine fibrillar structure. The correlation between age-related collagen changes, observed with texture analysis in normal tissue, was more pronounced in cancerous tissue. "Indeed, collagen fibrils appeared to be wavy or crimped in cancerous tissue; whereas, fibrils of older patients' normal tissue appeared diffuse, but still preserved a somewhat normal fine structure (Kirkpatrick et al., 2007). These wavy collagen fibrils were also demonstrated in high-grade serous (HGS) tumors of postmenopausal women, described in a study by Tilbury et al (Tilbury et al., 2017). They also demonstrated that in HGS tissue, the collagen fibers are dense and highly aligned, whereas in normal post-menopausal ovarian tissues the collagen network was more loose and mesh-like, which somewhat contradicts the findings of (Zhu et al., 1993) who described tightly arranged fibers in normal ovarian tissue. However, the latter publication was more than two decades prior to the findings of Tilbury *et al,* in addition to the fact that different visualization methods were used, suggesting that the results might not be entirely comparable. Overall, alterations in collagen organization are observed within benign to malignant transformation of ovarian tissue, however these results and interpretations seem less reliable since they are highly dependent on the visualization technique that is applied.

Pancreatic cancer. Pancreatic tumors are known to contain abundant collagenous stroma, which is produced by pancreatic stellate cells (PSC). These PSCs are not only significant for stroma formation, but also in facilitating cancer cell migration and invasion by reorganization of collagen fibers in response to hypoxia, immune evasion and therapeutic resistance (Pothula et al., 2020; Horioka et al., 2016). Drifka et al utilized SHG imaging to quantify collagen alterations in pancreatic ductal adenocarcinomas (PDAC) opposed to benign diseases. Regardless of an overall increase of fibrosis in PDAC, they did observe a heterogeneous appearance of collagen throughout the tissue microarray (TMA) cores, whereby PDAC collagen fibers were significantly longer ($p < 0.001$) and aligned ($p < 0.05$) than in normal tissue, which is consistent with other studies (Provenzano et al., 2006; Yuting et al., 2018; Tilbury et al., 2017; Brooks et al., 2016; Esbona et al., 2018; Ling et al., 2017). However, the degree of alignment was not correlated to the histological grade (Drifka et al., 2015). To further explore the clinical (survival) implications of collagen alignment in PDAC, an additional study was performed wherein was determined if collagen alignment could serve as a prognostic marker. Corresponding to previous results, stromal collagen was more aligned around PDAC cells compared to the more random organization around normal tissue ($p < 0.05$). Furthermore, an association between histological grade and alignment was yet again ruled out ($p=0.301$). High alignment did validate as a negative prognosticator of overall survival (OS), independent of traditional prognostic factors ($p=0.015$). Hereafter, the authors proceeded to investigate the significance of collagen organization with respect to cancer cell migration. By quantifying PDAC tissue cores for E-cadherin/vimentin double positivity, they observed a significant correlation between the epithelial–mesenchymal transition (EMT) expression by PDAC cells and collagen alignment (Spearman $r=0.202$; $p = 0.031$). Moreover, alignment was also positively correlated to α-SMA (Spearman $r=0.121$; $p = 0.022$) and syndecan-1 expression (Spearman $r=0.115$; $p = 0.029$), both markers of cancer-associated fibroblasts, which play a crucial role in remodeling of the tumor microenvironment (Drifka et al., 2016b). Enhanced α-SMA expression was also observed in a study investigating collagen reorganization in gastric cancer (Zhou et al., 2017). Using picrosirius red and IHC staining, the authors found an increase of collagen deposition, as well as a thicker appearance of fibers in gastric cancer versus non-neoplastic tissue, consistent with findings in other cancers (Esbona et al., 2018; Natal et al., 2018). In order to quantitively characterize fiber alterations, five features (i.e. alignment, length, width, density and straightness) were determined by SHG imaging. Within gastric cancer, a significant increase was observed with respect to alignment, length, straightness, width ($p < 0.05$) and

density ($p < 0.001$). However, only fiber length, density and width validated as prognosticators of OS, with collagen width being the most powerful of all (AUC 0.741; $p < 0.001$) (Zhou et al., 2017).

Colorectal and esophageal cancer. For colorectal cancer (CRC), the studies on collagen alignment are quite limited. In 2013, Liu et al performed an exploratory analysis ($n = 14$) in colon cancer tissue, applying MPM and SHG/TPEF imaging. Despite the limited sample size, they did observe distinct changes between normal versus cancerous mucosa, namely with disordered, elongated and sparsely visible collagen content in the latter (Liu et al., 2013). Hanley et al evaluated a stage I/II CRC cohort ($n = 64$) and found that increased collagen length, contrary to fiber alignment ($p = 0.067$), predicted a worse cancer-specific survival (HR 2.28; 95% CI 1.040–5.007; $p = 0.034$), which was consistent with their findings in esophageal adenocarcinoma (EAC ($n = 146$)) and head & neck squamous cell carcinoma (HNSCC ($n = 213$)) (Hanley et al., 2016). Among the few others researching colorectal cancer, Burke et al found that in stage I CRC ($n = 69$), an increased F/B was also a significant prognosticator for poor OS ($p = 0.03$) (Burke et al., 2015b). In accordance to aforementioned findings,(Hanley et al., 2016) Mellone et al similarly observed the prognostic quality of elongated collagen fibers in EAC ($n = 121$; $p = 0.028$) (Mellone et al., 2016), while for organization, others demonstrated a broad interfiber spacing as well as random distribution of fiber orientations in neoplastic esophageal stroma (Zhuo et al., 2009).

Squamous cell cancers. Several studies have explored changes in collagen fiber organization in squamous cell cancers (SCC) of the oral cavity and/or head and neck region. Previously, we briefly discussed the prognostic relevance of collagen organizational parameters in HNSCC, noting that fiber length could predict cancer survival, contrary to alignment (Hanley et al., 2016). This was also observed by Mellone et al ($n = 113$; $p = 0.027$) (Mellone et al., 2016). Devendra and colleagues contradict the aforementioned, since they report that not fiber length, but density ($n = 29$) was most significantly correlated to the clinicopathological parameters (i.e. tumor size ($p = 0.047$), TNM stage ($p = 0.016$) and lymph node metastasis ($p = 0.026$)). Whereas for organization, a correlation to these parameters was yet again ruled out (Devendra et al., 2018). Solely focusing on imaging aspects, two independent groups (both $n = 50$) applying PSR-POL analysis, demonstrated a statistically significant different coloration ($p < 0.001$), orientation ($p = 0.002$) and packing ($p = 0.03$) of collagen fibers with progression of tumor dedifferentiation (Arun Gopinathan et al., 2015; Kardam et al., 2016). In an effort to explain the transformation to a random fiber orientation in poorly differentiated tumors, the authors hypothesized that this could be due to formation of abnormal (i.e. pathological) collagen and proteolytic activities associated with carcinogenesis (Kardam et al., 2016). Since the appearance of collagen architecture seems to alter with progression, one could wonder if these patterns can already be observed in pre-cancerous lesions like oral submucous fibrosis (OSF), a chronic progressive condition of the oropharyngeal cavity susceptible to malignant transformation (Aziz, 1997). With an ANN based analysis of TEM images of collagen fibers, derived from OSF tissue and normal submucosa, a feature vector was chosen to subsequently train the artificial neural network. Herewith, Paul et al ($n = 145$) and Mukherjee et al ($n = 145$) both illustrated that the computational classification method was able to correctly classify normal submucosa, from less and advanced OSF stages, indicating its potential as a clinical detection and staging tool for OSF (Mukherjee et al., 2006; Paul et al., 2005). Other rare oral conditions with clinically aggressive potential are odontogenic keratocysts and ameloblastic carcinomas, members of the spectrum of odontogenic lesions (Browne, 1975). Aggarwal et al and Kulkarni et al investigated whether specific collagen patterns could distinguish odontogenic cysts and predict the aggressive behavior. They demonstrated a predominant orange-red collagen fiber birefringence in odontogenic keratocysts, odontogenic tumors and dentigerous cysts versus a yellow-green appearance in radicular cysts and ameloblastoma. Indicating more loosely packed fibers in the latter and more tightly organized fibers in the former. Hereby recognizing a distinctive property, but not necessarily a prognostic one (Aggarwal and Saxena, 2011; Kulkarni et al., 2017).

Breast cancer. To date, the majority of collagen organization research has been performed in breast cancer. In 2011, Conklin et al set out to assess whether TACS-3, previously discovered to be associated with cancer progression in a mouse model (Provenzano et al., 2006), was present in human histopathological samples and if so, to establish whether this was correlated to survival outcomes. In a cohort of various invasive breast cancers ($n = 196$), they retrospectively confirmed local areas of TACS-3. To determine the association with survival outcomes, a three scores classifier was assembled. All three TACS-3 scores were associated with a decreased disease-free survival (DFS) and disease-specific survival (DSS), with hazard ratios > 3.0 for score 1 and 2. As the stringency increased (i.e. score 3 to 2 to 1), the significance level improved. In a multivariate Cox proportional hazard analysis, presence of TACS-3 confirmed to be an independent prognosticator for DFS and DSS, in addition to the variables tumor size, estrogen (ER)/progesterone (PR) status and node status. This indicates that quantification of collagen alignment, by means of TACS, has potential as survival predictor in breast cancer (Conklin et al., 2011). Inspired by these results, the authors set out to investigate if this altered collagen alignment was also present in earlier disease stages and could predict recurrence of disease. Using SHG imaging, collagen alignment was determined in 227 ductal carcinomas in situ (DCIS). Among these cases, $n = 36$ (16%) experienced a recurrence (18 DCIS, 16 invasive breast cancer, 2 unknown stage), $n = 16$ had contralateral recurrences (8 DCIS, 8 invasive) and $n = 18$ experienced ipsilateral recurrences (10 DCIS, 8 invasive). Compared to normal ducts, collagen fibers demonstrated a modest trend toward a more perpendicular angle in DCIS ($p = 0.058$), however collagen alignment scores did not predict recurrence (HR 1.25; 95% CI 0.84–1.87; $p = 0.27$). However, TACS was more common in DCIS with features associated with poor prognosis (i.e. ER, PR, HER2 status and comedo necrosis) (Conklin et al., 2018).

In order to investigate the compositional changes of ECM throughout the process of collagen reorganization and carcinogenesis, Tomko et al identified 27 significantly altered ECM proteins between IDC and normal tissue ($n = 19$), of which 24 proteins (19 positive, 5 negative) correlated to fiber alignment scores. Amongst these, four ECM proteins (i.e. COL12A1, fibronectin, thrombospondin-2 and tenascin-C) correlated with poor distant metastasis-free survival. Using SHG imaging, the authors subsequently revealed that solely thrombospondin-2 and tenascin-C co-localized in the TACS-3 phenotype and formed fiber structures directly alongside straight collagen fibers in IDC ($p = 0.05$; $p = 0.01$), suggesting possible involvement in collagen fiber re-organization during tumorigenesis (Tomko et al., 2018). Prior to this research, Burke et al ruled out changes in F/B ratio and consequently also in fibrillar microstructure of DCIS ($n = 20$) compared to healthy tissue ($n = 37$), contrary to invasive carcinomas ($n = 147$), where alterations in F/B ratio and microstructure were observed. As IDC progressed to more dedifferentiated states (resp. $n = 8_{\text{grade 1}}$, $n = 88_{\text{grade 2}}$, $n = 15_{\text{grade 3}}$), the SHG F/B ratio correspondingly became significantly different. Similar to IDC, in invasive lobular carcinoma collagen microstructure was also altered, as indicated by a decrease of the F/B ratio compared to healthy tissue. Though in lobular carcinoma in situ, the F/B ratio was significantly different from healthy tissue, while in DCIS this was not, which is consistent with the different tumor behavior of both diseases (Burke et al., 2013).

Focusing on evolving the imaging techniques, Bredfelt et al developed a computational semi-automated protocol to determine an algorithmic model for TACS-3 analysis on TMAs, based on previous results

from Conklin et al, relating manually quantitated collagen reorganization to survival outcomes in breast cancer (Conklin et al., 2011). The results of the automated method had a positive correlation with all three manual scoring methods. In accordance, the TACS-3 negative patients had a significantly better DFS (HR 2.59; $p = 0.002$) and DSS (HR 2.25; $p = 0.008$) (Bredfeldt et al., 2014). Hereby validating the results from Conklin et al and illustrating the potential for application of semi-automated TACS-analysis as a clinical diagnostic tool, which allows for more consistent and detailed data collection. Applied in another study, this system confirmed that perpendicular collagen alignment to the tumor boundary TACS-3 (HR 1.65; $p = 0.049$) and TACS-2/TACS-3 (HR 1.24; $p = 0.037$) were predictors of poor patient OS in invasive breast cancer (IBC ($n = 371$)). Remarkably, local collagen density ($p = 0.047$) and alignment ($p = 0.007$) were associated with a better prognosis. Multivariate analysis validated localized collagen alignment (without consideration to angle) as an independent protective prognosticator (HR 0.05; 95% CI 0.00–0.48; $p = 0.01$), whereas TACS-3 was borderline non-significant as independent prognosticator for poor OS (HR 1.72; 95% CI 0.97–3.07; $p = 0.066$) (Esbona et al., 2018). While the abovementioned system reports promising results, it does require acquisition of additional tissue images. Therefore, others have developed more cost-effective methods which use clinically acquired H&E slides. For instance, Reis et al demonstrated the ability of an automated method based on BIF and LBP in combination with a random decision tree classifier, to correctly classify a set of IBC ($n = 52$) in the categories aligned or disorganized stroma with an accuracy of 84% (Reis et al., 2017). Also using H&E slides but combined with SHG imaging, Natal et al demonstrated within luminal type breast cancer, that collagen density ($p < 0.001$), quantity ($p < 0.001$) and organization ($p < 0.006$) are significantly more present in peritumoral regions opposed to intratumoral. In addition to this, for the former two parameters a strong correlation was observed between peri- and intratumoral areas ($r = 0.614$; $p < 0.001$), whereas for collagen organization, this was not observed ($r = 0.101$; $p = 0.479$). Intratumoral areas displayed a greater variation in orientation of collagen fibers. Interestingly, when evaluating the prognostic power of the aforementioned collagen parameters, this was only observed within intratumoral regions. A higher intratumoral density (HR 3.20; $p = 0.009$) and quantity (HR 4.127; $p = 0.031$) predicted relapse in univariate analyses, however adjusted in the multivariate analysis this power was lost. Solely for OS, intratumoral quantity remained prognostic in both analyses (HR 7.84; $p = 0.017$, $p_{adj} = 0.031$). Collagen organization did not display any value as prognosticator, neither for relapse-free survival ($p = 0.765$), nor for OS ($p = 0.440$) (Natal et al., 2018). Applying a manual method (for details, see section visual microscopy), Dekker et al were one of the first to demonstrate the predictive quality of collagen alignment in stage II/III breast cancer patients ($n = 175$) treated with neoadjuvant chemotherapy. They revealed that tumors with aligned stroma showed better response to neoadjuvant therapy compared to tumors with disorganized stroma ($p < 0.002$), but also were more likely to have lymph node metastasis (Dekker et al., 2015). This supports the hypothesis that tumor cells are more likely to migrate alongside aligned collagen fibers (Provenzano et al., 2006). In an effort to predict metastatic outcome, Burke et al explored the feasibility of intensity-based SHG F/B and fast Fourier transform analysis in breast cancer. They found that within untreated ER + tumors ($n = 125$) an increasing ln(F/B) was associated with longer metastatic-free survival (HR 0.16; 95% CI 0.05–0.55; $p = 0.004$), however this was borderline non-significant for OS (HR 0.28; 95% CI 0.07–1.10; $p = 0.068$). Since a subset of the cohort ($n = 60$) experienced metastasis, the authors proceeded to investigate whether the F/B of the primary tumor could predict response to tamoxifen. Interestingly, they observed a trend opposite to the aforementioned, since now a lower primary tumor F/B was significantly associated with slower disease progression (HR 3.39;95% CI 1.22–9.37; $p = 0.019$) (Burke et al., 2015b).

Urogenital cancers. In urogenital carcinomas, several studies with divers methods have been published over the years. Using GLEM texture analysis, one group retrospectively demonstrated that within higher grades of treatment-resistant prostate adenocarcinomas (CRPC ($n = 75$)) the collagen matrix was more disorganized, reflecting in a significantly higher entropy compared to benign prostate conditions ($p < 0.05$) (Jia et al., 2014). However, these results contradict the findings of Ling et al who demonstrated more aligned collagen within malignant prostate biopsies compared to normal tissue ($n = 24$), which corresponds with results in other solid tumors applying SHG (Hanley et al., 2016; Drifka et al., 2015; Provenzano et al., 2006; Esbona et al., 2018), a method which relies on detailed fiber organization whereas GLEM analysis provides a quasi-quantitive estimate of reactive stroma. Furthermore, in the study from Ling et al the anisotropic to isotropic ratio (A:I ratio; i.e. a parameter to compute regularity of fiber orientation) increased with a higher Gleason score. Using SHG imaging, they illustrated that CRPC consisted of a reticular pattern instead of a papillary one. However, with uncontrolled proliferation, as seen in highly aggressive CRPC, this pattern disappeared due to loss of SHG signal between the glands as a consequence of basement membrane destruction and accompanied influx of cancer cells in the glands and stroma (Ling et al., 2017). These results were later validated in a study with a larger cohort ($n = 42$) (Yuting et al., 2018), suggesting that this approach might assist in a more accurate characterization of CRPC. Consistent with the aligned fiber orientation in CRPC, in a cohort ($n = 189$) of non-muscle invasive bladder cancer it was demonstrated that tumor progression was yet again associated with more aligned collagen fibers ($p = 0.0018$) (Brooks et al., 2016).

Brain cancers. In a glioblastoma study, the authors distinguished two groups; one with a typical fibrillar collagen appearance ($n = 74$) with significantly shorter fibers angles, longer fibers and a more organized and aligned appearance and another with atypical fibrillar collagen ($n = 37$). Remarkably, the organized collagen signature demonstrated a significantly better survival ($p = 0.001$), which maintained significance in the multivariate analysis ($p = 0.032$) (Pointer et al., 2017).

3. Conclusion

With this review we give a comprehensive overview of literature on the topic of stromal collagen organization in cancer tissue. In summary, we conclude that various standardized visualization methods are currently available for characterization of the collagen architecture, but literature is limited on providing a head-to-head comparison between the different techniques with respect to implementation, time- and cost-effectiveness Therefore, no “golden standard” is currently available. Collagen organization contains valuable information with regard to metastatic potential and clinical outcomes in cancer. However, the significance of an aligned versus disorganized collagen morphology differs between cancer types. We should consider the possibility that this biomarker is only applicable in certain cancers, likewise to other conventional biomarkers (e.g., *KRAS* in CRC). Since the tumor microenvironment is a very heterogeneous phenomenon with distinct characterizations between cancers, future research into intercellular signaling could perhaps provide more insight in the discrepancies we observed. Further research is therefore necessary, before any steps can be made towards clinical implementation.

Funding

This research received funding from “Genootschap Landgoed Keukenhof”. The funders had no role in study design, data collection and analysis, decision to publish, or preparation of the manuscript.

Authors contributions

Conception, design and interpretation of data: SZ
Writing and final approval of the manuscript: SZ, HG, RT, WE

Declaration of Competing Interest

All authors declare no conflicts of interest.

Acknowledgements

The authors would like to give special thanks to Jan Schoones for his efforts and assistance in the execution of the literature search.

Appendix A. Supplementary data

Supplementary material related to this article can be found, in the online version, at doi:https://doi.org/10.1016/j.critrevonc.2020.102907.

References

Aggarwal, P., Saxena, S., 2011. Stromal differences in odontogenic cysts of a common histopathogenesis but with different biological behavior: a study with picrosirius red and polarizing microscopy. Indian J. Cancer 48, 211–215.
Arun Gopinathan, P., Kokila, G., Jyothi, M., Ananjan, C., Pradeep, L., Humaira Nazir, S., 2015. Study of collagen birefringence in different grades of oral squamous cell carcinoma using picrosirius red and polarized light microscopy. Scientifica (Cairo) 2015 802980.
Aziz, S.R., 1997. Oral submucous fibrosis: an unusual disease. J. N. J. Dent. Assoc. 68, 17–19.
Barcus, C.E., O'Leary, K.A., Brockman, J.L., Rugowski, D.E., Liu, Y., Garcia, N., Yu, M., Keely, P.J., Eliceiri, K.W., Schuler, L.A., 2017. Elevated collagen-I augments tumor progressive signals, intravasation and metastasis of prolactin-induced estrogen receptor alpha positive mammary tumor cells. Breast Cancer Res. 19, 9.
Barczyk, M., Carracedo, S., Gullberg, D., 2010. Integrins. Cell Tissue Res. 339, 269–280.
Bloembergen, N., 1965. Nonlinear Optics. W.A. Benjamin Inc.
Bray, F., Ferlay, J., Soerjomataram, I., Siegel, R.L., Torre, L.A., Jemal, A., 2018. Global Cancer statistics 2018: GLOBOCAN estimates of incidence and mortality worldwide for 36 cancers in 185 countries. CA Cancer J. Clin.
Bredfeldt, J.S., Liu, Y., Conklin, M.W., Keely, P.J., Mackie, T.R., Eliceiri, K.W., 2014. Automated quantification of aligned collagen for human breast carcinoma prognosis. J. Pathol. Inform. 5, 28.
Brooks, M., Mo, Q., Krasnow, R., Ho, P.L., Lee, Y.C., Xiao, J., Kurtova, A., Lerner, S., Godoy, G., Jian, W., Castro, P., Chen, F., Rowley, D., Ittmann, M., Chan, K.S., 2016. Positive association of collagen type I with non-muscle invasive bladder cancer progression. Oncotarget 7, 82609–82619.
Browne, R.M., 1975. The pathogenesis of odontogenic cysts: a review. J. Oral Pathol. 4, 31–46.
Burke, K., Tang, P., Brown, E., 2013. Second harmonic generation reveals matrix alterations during breast tumor progression. J. Biomed. Opt. 18, 31106.
Burke, K.A., Dawes, R.P., Cheema, M.K., Van Hove, A., Benoit, D.S., Perry, S.W., Brown, E., 2015a. Second-harmonic generation scattering directionality predicts tumor cell motility in collagen gels. J. Biomed. Opt. 20, 051024.
Burke, K., Smid, M., Dawes, R.P., Timmermans, M.A., Salzman, P., van Deurzen, C.H., Beer, D.G., Foekens, J.A., Brown, E., 2015b. Using second harmonic generation to predict patient outcome in solid tumors. BMC Cancer 15, 929.
Butcher, D.T., Alliston, T., Weaver, V.M., 2009. A tense situation: forcing tumour progression. Nat. Rev. Cancer 9, 108–122.
Chen, Y., Terajima, M., Yang, Y., Sun, L., Ahn, Y.H., Pankova, D., Puperi, D.S., Watanabe, T., Kim, M.P., Blackmon, S.H., Rodriguez, J., Liu, H., Behrens, C., Wistuba, I.I., Minelli, R., Scott, K.L., Sanchez-Adams, J., Guilak, F., Pati, D., Thilaganathan, N., Burns, A.R., Creighton, C.J., Martinez, E.D., Zal, T., Grande-Allen, K.J., Yamauchi, M., Kurie, J.M., 2015. Lysyl hydroxylase 2 induces a collagen cross-link switch in tumor stroma. J. Clin. Invest. 125, 1147–1162.
Conklin, M.W., Eickhoff, J.C., Riching, K.M., Pehlke, C.A., Eliceiri, K.W., Provenzano, P.P., Friedl, A., Keely, P.J., 2011. Aligned collagen is a prognostic signature for survival in human breast carcinoma. Am. J. Pathol. 178, 1221–1232.
Conklin, M.W., Gangnon, R.E., Sprague, B.L., Van Gemert, L., Hampton, J.M., Eliceiri, K.W., Bredfeldt, J.S., Liu, Y., Surachaicharn, N., Newcomb, P.A., Friedl, A., Keely, P.J., Trentham-Dietz, A., 2018. Collagen alignment as a predictor of recurrence after ductal carcinoma in situ. Cancer Epidemiol. Biomarkers Prev. 27, 138–145.
Dayhoff, J.E., DeLeo, J.M., 2001. Artificial neural networks: opening the black box. Cancer 91, 1615–1635.
Dekker, T.J., Charehbili, A., Smit, V.T., ten Dijke, P., Kranenbarg, E.M., van de Velde, C.J., Nortier, J.W., Tollenaar, R.A., Mesker, W.E., Kroep, J.R., 2015. Disorganised stroma determined on pre-treatment breast cancer biopsies is associated with poor response to neoadjuvant chemotherapy: results from the NEOZOTAC trial. Mol. Oncol. 9, 1120–1128.
Denk, W., Svoboda, K., 1997. Photon upmanship: why multiphoton imaging is more than a gimmick. Neuron 18, 351–357.
Denk, W., Strickler, J.H., Webb, W.W., 1990. Two-photon laser scanning fluorescence microscopy. Science 248, 73–76.
Desgrosellier, J.S., Cheresh, D.A., 2010. Integrins in cancer: biological implications and therapeutic opportunities. Nat. Rev. Cancer 10, 9–22.
Devendra, A., Niranjan, K.C., Swetha, A., Kaveri, H., 2018. Histochemical analysis of collagen reorganization at the invasive front of oral squamous cell carcinoma tumors. J. Investig. Clin. Dent. 9.
Dolino, G., 1973. Direct observation of DauphineÂ twins in quartz with second-harmonic light. Appl. Phys. Lett. 623–625.
Drifka, C.R., Tod, J., Loeffler, A.G., Liu, Y., Thomas, G.J., Eliceiri, K.W., Kao, W.J., 2015. Periductal stromal collagen topology of pancreatic ductal adenocarcinoma differs from that of normal and chronic pancreatitis. Mod. Pathol. 28, 1470–1480.
Drifka, C.R., Loeffler, A.G., Mathewson, K., Mehta, G., Keikhosravi, A., Liu, Y., Lemancik, S., Ricke, W.A., Weber, S.M., Kao, W.J., Eliceiri, K.W., 2016a. Comparison of picrosirius red staining with second harmonic generation imaging for the quantification of clinically relevant collagen Fiber Features in histopathology samples. J. Histochem. Cytochem. 64, 519–529.
Drifka, C.R., Loeffler, A.G., Mathewson, K., Keikhosravi, A., Eickhoff, J.C., Liu, Y., Weber, S.M., Kao, W.J., Eliceiri, K.W., 2016b. Highly aligned stromal collagen is a negative prognostic factor following pancreatic ductal adenocarcinoma resection. Oncotarget 7, 76197–76213.
Dvorak, H.F., 2015. Tumors: wounds that do not heal-redux. Cancer Immunol. Res. 3, 1–11.
Esbona, K., Yi, Y., Saha, S., Yu, M., Van Doorn, R.R., Conklin, M.W., Graham, D.S., Wisinski, K.B., Ponik, S.M., Eliceiri, K.W., Wilke, L.G., Keely, P.J., 2018. The Presence of Cyclooxygenase 2, Tumor-Associated Macrophages, and Collagen Alignment as Prognostic Markers for Invasive Breast Carcinoma Patients. Am. J. Pathol. 188, 559–573.
Franken, P.A., 1961. Generation of optical harmonics. Phys. Rev. Lett. 7, 118–119.
Freund, I., Deutsch, M., Sprecher, A., 1986. Connective tissue polarity. Optical second-harmonic microscopy, crossed-beam summation, and small-angle scattering in rat-tail tendon. Biophys. J. 50, 693–712.
Friedl, P., Maaser, K., Klein, C.E., Niggemann, B., Krohne, G., Zanker, K.S., 1997. Migration of highly aggressive MV3 melanoma cells in 3-dimensional collagen lattices results in local matrix reorganization and shedding of alpha2 and beta1 integrins and CD44. Cancer Res. 57, 2061–2070.
Gannaway, J., Sheppard, C.J.R., 1978. Second-harmonic imaging in the scanning optical microscope. Opt. Quantum Electron. 10, 435–439.
Gilkes, D.M., Bajpai, S., Chaturvedi, P., Wirtz, D., Semenza, G.L., 2013. Hypoxia-inducible factor 1 (HIF-1) promotes extracellular matrix remodeling under hypoxic conditions by inducing P4HA1, P4HA2, and PLOD2 expression in fibroblasts. J. Biol. Chem. 288, 10819–10829.
Goeppert-Mayer, M., 1931. Ueber elementarakte mit Zwei Quantenspruengen. Ann. Phys. (Paris) 9, 273.
Hanahan, D., Coussens, L.M., 2012. Accessories to the crime: functions of cells recruited to the tumor microenvironment. Cancer Cell 21, 309–322.
Hanahan, D., Weinberg, R.A., 2000. The hallmarks of cancer. Cell 100, 57–70.
Hanahan, D., Weinberg, R.A., 2011. Hallmarks of cancer: the next generation. Cell 144, 646–674.
Hanley, C.J., Noble, F., Ward, M., Bullock, M., Drifka, C., Mellone, M., Manousopoulou, A., Johnston, H.E., Hayden, A., Thirdborough, S., Liu, Y., Smith, D.M., Mellows, T., Kao, W.J., Garbis, S.D., Mirnezami, A., Underwood, T.J., Eliceiri, K.W., Thomas, G.J., 2016. A subset of myofibroblastic cancer-associated fibroblasts regulate collagen fiber elongation, which is prognostic in multiple cancers. Oncotarget 7, 6159–6174.
Horioka, K., Ohuchida, K., Sada, M., Zheng, B., Moriyama, T., Fujita, H., Manabe, T., Ohtsuka, T., Shimamoto, M., Miyazaki, T., Mizumoto, K., Oda, Y., Nakamura, M., 2016. Suppression of CD51 in pancreatic stellate cells inhibits tumor growth by reducing stroma and altering tumor-stromal interaction in pancreatic cancer. Int. J. Oncol. 48, 1499–1508.
Jia, X., Sun, Y., Wang, B., 2014. Gray level entropy matrix is a superior predictor than multiplex ELISA in the detection of reactive stroma and metastatic potential of high-grade prostatic adenocarcinoma. IUBMB Life 66, 847–853.
Kardam, P., Mehendiratta, M., Rehani, S., Kumra, M., Sahay, K., Jain, K., 2016. Stromal fibers in oral squamous cell carcinoma: A possible new prognostic indicator? J. Oral Maxillofac. Pathol. 20, 405–412.
Keely, P.J., 2011. Mechanisms by which the extracellular matrix and integrin signaling act to regulate the switch between tumor suppression and tumor promotion. J. Mammary Gland Biol. Neoplasia 16, 205–219.
Kirkpatrick, N.D., Brewer, M.A., Utzinger, U., 2007. Endogenous optical biomarkers of ovarian cancer evaluated with multiphoton microscopy. Cancer Epidemiol. Biomarkers Prev. 16, 2048–2057.
Kulkarni, P.G., Kumari, M.A., Jahagirdar, A., Nandan, S., Reddy, D.S., Keerthi, M., 2017. Collagen and its role in predicting the biological behavior of odontogenic lesions. J. Contemp. Dent. Pract. 18, 137–141.
Lepzelter, D., Zaman, M.H., 2014. Modeling persistence in mesenchymal cell motility using explicit fibers. Langmuir 30, 5506–5509.
Ling, Y., Li, C., Feng, K., Palmer, S., Appleton, P.L., Lang, S., McGloin, D., Huang, Z., Nabi, G., 2017. Second harmonic generation (SHG) imaging of cancer heterogeneity in ultrasound guided biopsies of prostate in men suspected with prostate cancer. J. Biophotonics 10, 911–918.
Liotta, L.A., Kohn, E.C., 2001. The microenvironment of the tumour-host interface. Nature 411, 375–379.
Liu, N., Chen, J., Xu, R., Jiang, S., Xu, J., Chen, R., 2013. Label-free imaging characteristics of colonic mucinous adenocarcinoma using multiphoton microscopy. Scanning

35, 277–282.
Malik, R., Luong, T., Cao, X., Han, B., Shah, N., Franco-Barraza, J., Han, L., Shenoy, V.B., Lelkes, P.I., Cukierman, E., 2018. Rigidity controls human desmoplastic matrix anisotropy to enable pancreatic cancer cell spread via extracellular signal-regulated kinase 2. Matrix Biol.
Marcos-Garces, V., Harvat, M., Molina Aguilar, P., Ferrandez Izquierdo, A., Ruiz-Sauri, A., 2017. Comparative measurement of collagen bundle orientation by Fourier analysis and semiquantitative evaluation: reliability and agreement in Masson's trichrome, Picrosirius red and confocal microscopy techniques. J. Microsc. 267, 130–142.
Mellone, M., Hanley, C.J., Thirdborough, S., Mellows, T., Garcia, E., Woo, J., Tod, J., Frampton, S., Jenei, V., Moutasim, K.A., Kabir, T.D., Brennan, P.A., Venturi, G., Ford, K., Herranz, N., Lim, K.P., Clarke, J., Lambert, D.W., Prime, S.S., Underwood, T.J., Vijayanand, P., Eliceiri, K.W., Woelk, C., King, E.V., Gil, J., Ottensmeier, C.H., Thomas, G.J., 2016. Induction of fibroblast senescence generates a non-fibrogenic myofibroblast phenotype that differentially impacts on cancer prognosis. Aging (Albany NY) 9, 114–132.
Mohler, W., Millard, A.C., Campagnola, P.J., 2003. Second harmonic generation imaging of endogenous structural proteins. Methods 29, 97–109.
Mukherjee, A., Paul, R.R., Chaudhuri, K., Chatterjee, J., Pal, M., Banerjee, P., Mukherjee, K., Banerjee, S., Dutta, P.K., 2006. Performance analysis of different wavelet feature vectors in quantification of oral precancerous condition. Oral Oncol. 42, 914–928.
Natal, R.A., Vassallo, J., Paiva, G.R., Pelegati, V.B., Barbosa, G.O., Mendonca, G.R., Bondarik, C., Derchain, S.F., Carvalho, H.F., Lima, C.S., Cesar, C.L., Sarian, L.O., 2018. Collagen analysis by second-harmonic generation microscopy predicts outcome of luminal breast cancer. Tumour Biol. 40 1010428318770953.
Navab, R., Strumpf, D., To, C., Pasko, E., Kim, K.S., Park, C.J., Hai, J., Liu, J., Jonkman, J., Barczyk, M., Bandarchi, B., Wang, Y.H., Venkat, K., Ibrahimov, E., Pham, N.A., Ng, C., Radulovich, N., Zhu, C.Q., Pintilie, M., Wang, D., Lu, A., Jurisica, I., Walker, G.C., Gullberg, D., Tsao, M.S., 2016. Integrin alpha11beta1 regulates cancer stromal stiffness and promotes tumorigenicity and metastasis in non-small cell lung cancer. Oncogene 35, 1899–1908.
Nielssen, B., Allbregtsen, F., Danielsen, H.E., 2008. Statistical nuclear texture analysis in Cancer research: a review of methods and applications. Crit. Rev. Oncog. 14, 89–164.
Paul, R.R., Mukherjee, A., Dutta, P.K., Banerjee, S., Pal, M., Chatterjee, J., Chaudhuri, K., Mukkerjee, K., 2005. A novel wavelet neural network based pathological stage detection technique for an oral precancerous condition. J. Clin. Pathol. 58, 932–938.
Phillips, R.J., 1989. Hindered transport of spherical macromolecules in fibrous membranes and gels. AIChE 35, 1761–1769.
Pointer, K.B., Clark, P.A., Schroeder, A.B., Salamat, M.S., Eliceiri, K.W., Kuo, J.S., 2017. Association of collagen architecture with glioblastoma patient survival. J. Neurosurg. 126, 1812–1821.
Pothula, S.P., Pirola, R.C., Wilson, J.S., Apte, M.V., 2020. Pancreatic stellate cells: aiding and abetting pancreatic cancer progression. Pancreatology.
Prockop, D.J., Kivirikko, K.I., Tuderman, L., Guzman, N.A., 1979. The biosynthesis of collagen and its disorders (first of two parts). N. Engl. J. Med. 301, 13–23.
Provenzano, P.P., Eliceiri, K.W., Campbell, J.M., Inman, D.R., White, J.G., Keely, P.J., 2006. Collagen reorganization at the tumor-stromal interface facilitates local invasion. BMC Med. 4, 38.
Provenzano, P.P., Inman, D.R., Eliceiri, K.W., Knittel, J.G., Yan, L., Rueden, C.T., White, J.G., Keely, P.J., 2008. Collagen density promotes mammary tumor initiation and progression. BMC Med. 6, 11.
Reis, S., Gazinska, P., Hipwell, J.H., Mertzanidou, T., Naidoo, K., Williams, N., Pinder, S., Hawkes, D.J., 2017. Automated classification of breast Cancer stroma maturity from histological images. IEEE Trans. Biomed. Eng. 64, 2344–2352.
Ribatti, D., Tamma, R., 2018. A revisited concept. Tumors: Wounds that do not heal. Crit. Rev. Oncol. Hematol. 128, 65–69.
Riching, K.M., Cox, B.L., Salick, M.R., Pehlke, C., Riching, A.S., Ponik, S.M., Bass, B.R., Crone, W.C., Jiang, Y., Weaver, A.M., Eliceiri, K.W., Keely, P.J., 2014. 3D collagen alignment limits protrusions to enhance breast cancer cell persistence. Biophys. J. 107, 2546–2558.
Rittie, L., 2017. Method for picrosirius red-polarization detection of collagen fibers in tissue sections. Methods Mol. Biol. 1627, 395–407.
Stylianopoulos, T., Diop-Frimpong, B., Munn, L.L., Jain, R.K., 2010. Diffusion anisotropy in collagen gels and tumors: the effect of fiber network orientation. Biophys. J. 99, 3119–3128.
Tilbury, K.B., Campbell, K.R., Eliceiri, K.W., Salih, S.M., Patankar, M., Campagnola, P.J., 2017. Stromal alterations in ovarian cancers via wavelength dependent Second Harmonic Generation microscopy and optical scattering. BMC Cancer 17, 102.
Tomko, L.A., Hill, R.C., Barrett, A., Szulczewski, J.M., Conklin, M.W., Eliceiri, K.W., Keely, P.J., Hansen, K.C., Ponik, S.M., 2018. Targeted matrisome analysis identifies thrombospondin-2 and tenascin-C in aligned collagen stroma from invasive breast carcinoma. Sci. Rep. 8, 12941.
Wang, S., Larin, K.V., 2015. Optical coherence elastography for tissue characterization: a review. J. Biophotonics 8, 279–302.
Watson, J.M., Marion, S.L., Rice, P.F., Bentley, D.L., Besselsen, D.G., Utzinger, U., Hoyer, P.B., Barton, J.K., 2014. In vivo time-serial multi-modality optical imaging in a mouse model of ovarian tumorigenesis. Cancer Biol. Ther. 15, 42–60.
Yuting, L., Li, C., Zhou, K., Guan, G., Appleton, P.L., Lang, S., McGloin, D., Huang, Z., Nabi, G., 2018. Microscale characterization of prostate biopsies tissues using optical coherence elastography and second harmonic generation imaging. Lab. Invest. 98, 380–390.
Zhou, Z.H., Ji, C.D., Xiao, H.L., Zhao, H.B., Cui, Y.H., Bian, X.W., 2017. Reorganized collagen in the tumor microenvironment of gastric Cancer and its association with prognosis. J. Cancer 8, 1466–1476.
Zhu, G.G., Stenback, F., Risteli, L., Risteli, J., Kauppila, A., 1993. Organization of type III collagen in benign and malignant ovarian tumors. An immunohistochemical study. Cancer 72, 1679–1684.
Zhuo, S., Chen, J., Xie, S., Hong, Z., Jiang, X., 2009. Extracting diagnostic stromal organization features based on intrinsic two-photon excited fluorescence and second-harmonic generation signals. J. Biomed. Opt. 14 020503.
https://www.histalim.com/home/activities/our-services/histology/masson-trichrome/. In.

Stéphanie M. Zunder PhD candidate from 2017 to 2019, currently 4th year resident Internal Medicine in Leiden University Medical Centre. Starting fellowship Medical Oncology in May 2020

Hans Gelderblom: Professor and head of the Medical Oncology department of the Leiden University Medical Center

Rob A. Tollenaar: Professor and head of the Surgery department of the Leiden University Medical Center

Wilma E. Mesker Assistant professor at the Department of Surgery. Research field focused on tumor-stroma interactions.